

Systematic onset of periodic patterns in random disks packings

Supplementary Material

Nikola Topic,¹ Thorsten Pöschel,^{1,2} and Jason A.C. Gallas^{1,2,3}

¹*Institute for Multiscale Simulation, Friedrich-Alexander-Universität Erlangen-Nürnberg, 91052 Erlangen, Germany*

²*Instituto de Altos Estudos da Paraíba, Rua Silvino Lopes 419-2502, 58039-190 João Pessoa, Brazil*

³*Complexity Sciences Center, 9225 Collins Avenue Suite 1208, Surfside, FL 33154, USA*

(Dated: March 2, 2018 at 14:45)

To check whether packings in channels with non-integer and integer widths are qualitatively different, we study the distribution of transients and periods in channels of non-integer but rational widths $w = 5.8$, $w = 6.2$, and irrational widths $w = 2\pi \simeq 6.2831\dots$ and $w = 10\sqrt{2} \simeq 14.1421\dots$ and compare the results with those in Fig. 4 and Fig. 5 of the manuscript. For these four non-integer channel widths we consistently found sediments to display periodic patterns.

The probability density function (PDF) of transient lengths seen in Fig. 1, sampled over 10^6 realizations, shows similar qualitative behavior as for integer widths. Most noticeably Fig. 1 shows the characteristic approximately exponential tail. The distribution of periods, Fig. 2, shows the characteristic peaks. Therefore, from these simulations we conclude that no qualitative difference exists between packings deposited in channels with integer, rational, or irrational widths.

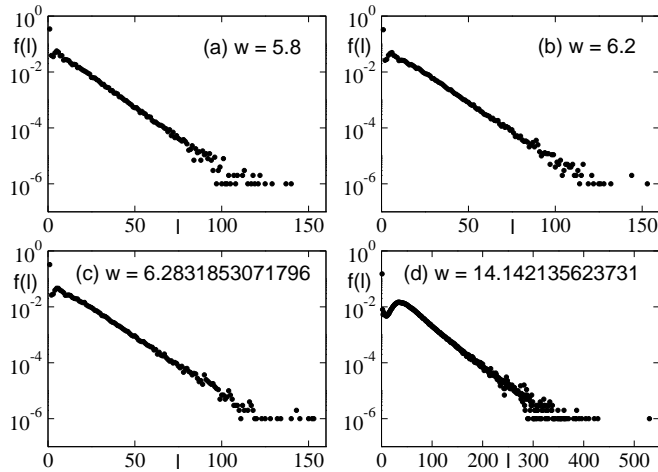


Figure 1. Probability density functions of transient lengths showing that non-integer channel widths produce similar results. The number of samples is 10^6 for each channel width.

In the packings discussed in the Letter, particles were dropped with uniform probability over the opening of the channel. Now, we consider the influence of the bottom layer, i.e. of the particles touching the ground. Two distinct scenarios of width 20 are considered: First, the bottom layer is formed by 20 particles of diameter 1 at positions $0.5 + i + \Delta_i$, $i = 0\dots 19$, where Δ_i are uniformly distributed real numbers in the range $[-0.1, 0.1]$, what causes overlaps between particles and particles and walls. However, although the initial layer is made artificially, this is not in contradiction with the

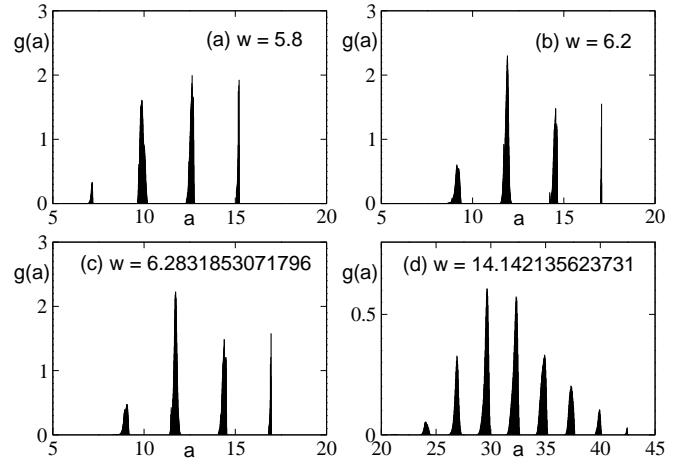


Figure 2. Probability density function of periods indicating that non-integer channel widths produce similar results. The number of samples is 10^6 for each channel width.

Visscher-Bolsterli algorithm. This is the "random shift" scenario. The corresponding PDFs for transient lengths and periods are shown in Figs. 3(a) and 3(c). Second, particles at the bottom layer were deposited having gaps between them distributed with uniform probability in the range $[0, 0.1]$. This is the "random separation" scenario. In this case there are less than 20 particles on the ground. The results for this experiment are shown in Figs. 3(b) and 3(d). Individual panels in Fig. 3 represent 10^5 system realizations.

As illustrated by Fig. 3, for both experiments described above the packings always become periodic and the PDFs of transient length and periods are similar to the case when the bottom layer is generated by random deposition, as discussed in the Letter. The transient distribution shows the exponential tail, while for periods we find approximately equidistant peaks, with top of peaks showing a bell-shaped profile – all qualitatively similar to the case of random deposition of particles.

In the Letter the focus is on the length of transients and periods. Here, we extend the analysis by considering packing fractions within the deposits. We first focus on how packing fraction depends on height, Fig. 4. As in the Letter, each particle is dropped with uniform probability over the opening of the container.

The packing fraction at certain height y_0 is defined as:

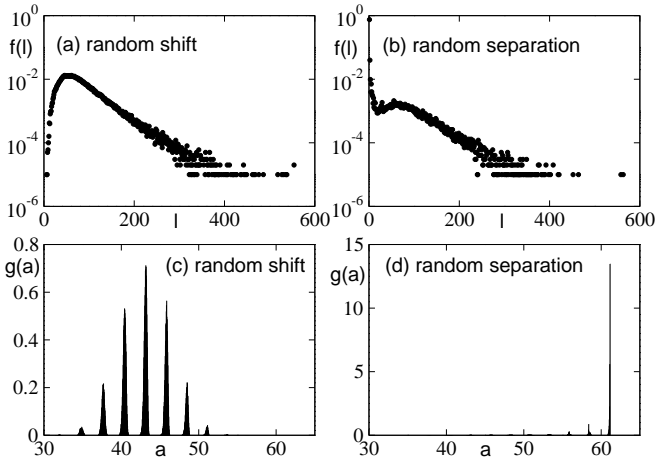


Figure 3. Experiments showing that distinct bottom layers (described in the text) produce quite similar results: (a) and (b) PDFs of transient lengths and (c) and (d) PDFs of periods.

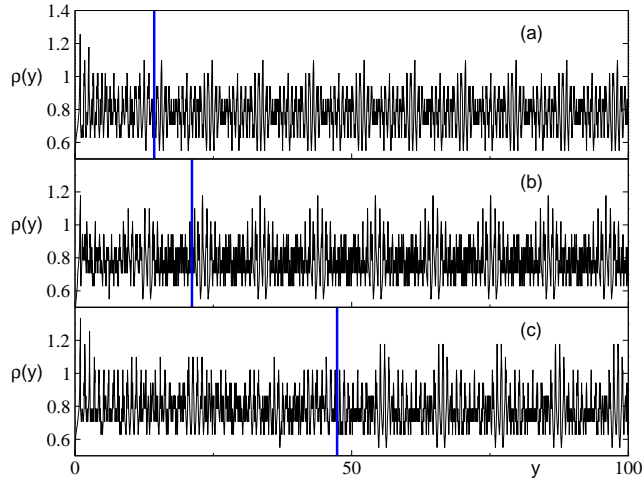


Figure 4. Dependence of the packing fraction, ρ , on height y for three system realization with $w = 20$. The blue vertical lines mark the end of the transient part of a packing.

$\rho(y_0) = n_{y_0} \pi d / (4w)$, where n_{y_0} is the number of particles that intersect the line $y = y_0$, and d is the diameter of particles, here $d = 1$. If there is a single particle in the system the total mass in the system is: $\int_0^{+\infty} \rho(y) w dy = \pi d^2 / 4$, i.e. the mass of a single particle, assuming the density of particles is unity. This shows that the packing fraction measure is well-defined. This measure of packing fraction can locally exceed 1. As expected, the packing fraction becomes a periodic function of height after the transient ends. Otherwise, no qualitative differences are discernible.

Next, we study PDFs of packing fractions in the transient and the periodic parts of packings. The packing fraction in the transient part of a single packing was defined as the fraction of the surface covered with particles between the ground and the center of the lowest particle of the periodic part of the packing. If a packing did not have a transient the packing fraction was

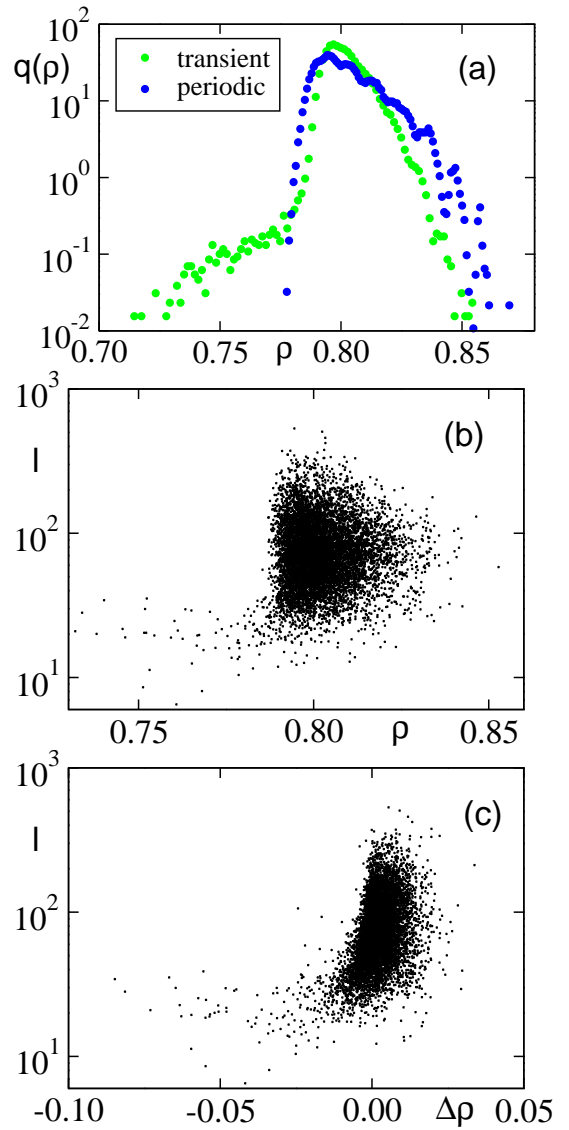


Figure 5. (a) Packing fraction PDF, $q(\rho)$, for the periodic and transient parts of packings. Each individual panel is derived from 10^4 system realizations with the channel width $w = 20$. (b) Dependence of the transient length, l , on the packing fraction. Here ρ is a packing fraction of the transient part. Each dot corresponds to a single system realization. (c) $\Delta\rho$ is a difference between packing fraction in the transient and the periodic part of the packing, i.e. $\Delta\rho = \rho_{\text{transient}} - \rho_{\text{periodic}}$.

not measured, which happened in about 10% of all deposits. For the periodic part, the packing fraction was measured between the center of the highest particle of the transient and the lowest particle of the surface of the packing.

Figure 5(a) shows the PDFs of packing fractions for transients and periodic patterns. The most prominent differences between the transient and periodic part of packings are: a) The PDF for periodic patterns shows near its peak an oscillatory behavior of clearly larger amplitude than for PDF of transients, and b) While the PDF of periodic patterns shows a sharp cut-off at around $\rho = 0.78$, the PDF of the transients

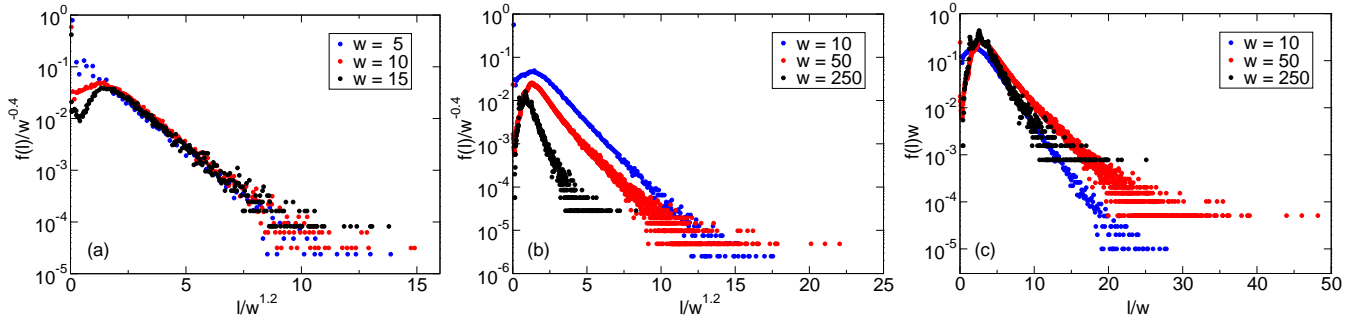


Figure 6. (a) Collapse of the data in Figs. 3 of the Letter. (b) Collapse of the data in Figs. 4 of the Letter, plotted as in (a). (c) Collapse of the data in Figs. 4 but plotted distinctly from (a) and (b).

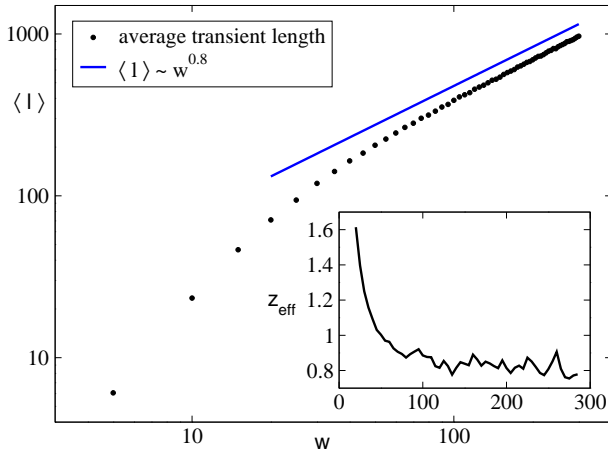


Figure 7. Dependence of the average transient length on the channel width. Inset: dependence of the effective dynamic exponent on the system width.

shows a slowly decaying tail down to about $\rho = 0.71$. Figures 5(b) and 5(c) illustrate attempts to show whether there is a correlation between the length of a transient and a packing fraction in the transient part, or the difference between pack-

ing fractions of the periodic and transient part. We find that the transient length correlates more with the difference of packing fractions between the transient and the periodic pattern, than with the packing fraction of the transient.

Figure 6(a) shows a collapse of the curves from Fig. 3 of the Letter while Figs. 6(b) and 6(c) illustrate two distinct representations of the data in Fig. 4 of the Letter. Figure 6(b) uses the same exponents as in Fig. 6(a) while in (c) a different exponent is used. While there is a reasonable collapse in Fig. 6(a), the data in panels (b) and (c) do not show good collapses.

Finally, Fig. 7 illustrates the dependence of the average transient length $\langle \ell \rangle$ on the channel width w , to check whether the system displays a *dynamical exponent*, say z , describing the temporal scaling required for the system to reach the stationary state as a function the system size, and that could be compared with other universality classes such as, e.g. the directed percolation. Here, transient lengths were averaged over 10,000 system realisations for each channel width. In the inset, the effective dynamic exponent, z_{eff} , was calculated by fitting a straight line through the set of points $[\log(w_i) \log(\langle \ell_i \rangle)]$, $i=1\dots 6$, where $w_i = w + i\Delta w$, with $\Delta w = 5$. Figure 7 provides an indication that a unique dynamical exponent may indeed emerge for larger systems which, however, are beyond our current computational capabilities.